BURIED (TABULAR) MASSIVE-ICE AND POSSIBLE PERIGLACIAL OVERBURDENS ON MARS. R.J. Soare[1].[1]Dept. of Geography, Dawson College, Montreal, Qc., Canada H3Z 1A4, rsoare@dawsoncollege.qc.ca.

Introduction: Recently, exposures of tabular, *m*assive water-*i*ce **[*MI*]** (decametres thick and buried shallowly) have been observed on scarp-faces in thermokarst-like depressions at the mid-latitudes of the two Martian hemispheres **[e.g. 1-3]** (**Fig. 1)**. The ***MI*** is thought to have originated as precipitated snow/ice that accumulated at the surface and was then buried beneath a combination of sublimation-driven lag and aeolian deposits **[e.g. 1-3]**.

Typically, the scarp floors, walls, overburdens and adjacent terrain are punctuated by polygonised terrain **(Fig. 1)**. Metres-deep thermokarst-like depressions that do not show exposed ice (not seen here) also dot the local/regional landscape.

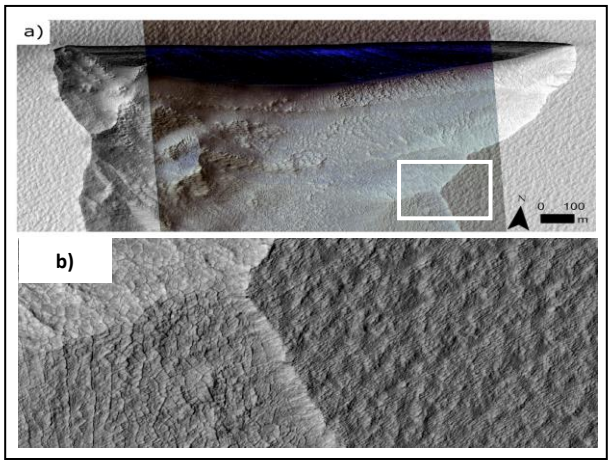

Fig. 1: (a) Nadir view of water-ice exposure ***(in blue)*** on a Promethei Terra scarp-face (enhanced-color *HiRISE* image ESP_057466_1230). The water-ice signature has been corroborated by ***CRISM*** spectral data **[1]**. Not seen here are metres-thick unconformities in the ice that run roughly parallel to one another and transversally with regard to the surface. (**b)** Close-up of three-different polygonised terrain morphologies within/adjacent to the scarp in **(a)**: **i.** low-centred (possible ice-wedge) polygons **[*LCPs*]** ~10-20 m in diameter on the lower left side of the image; **ii.** slightly larger high-centred (possibly ice-wedge) polygons ***[HCPs]*** to the right of **i;** and, **iii.** transitional polygons that become much blockier with proximity to the scarp face (not seen here). Polygon coverage is ubiquitous wherever there is no ice exposure. Not seen at this magnification/perspective is a metres-thick polygonised overburden that overlies the exposed ice. Image credits: *NASA*/*JPL*/University of Arizona.

Similar landscape assemblages are observed on Earth in the ice-rich permafrost, for example, of the *T*uktoyaktuk *C*oastlands **[*TC*]** of northern Canada **[e.g. 4-7]** and the Yamal Peninsula in eastern Russia **[e.g. 8]**. In both regions the glacial/periglacial cycling of water dates back from the present day to the mid- to late Wisconsinian Glacial Episode **[e.g. 4-6]**.

Here, we do two things: **1)** describe/discuss the exposures of tabular ***MI*** and overlying ice wedges in the ***TC***; and, **2)** compare/contrast this type of "*ice complex*" with the scarp-based (possible) ice complexes observed on Mars.

Fig. 2. Cross-sectional view of tabular ***MI*** at *P*eninsula *P*oint **[*PP*]**, ~6 km SW of Tuktoyaktuk, *NWT*, Canada The observed ice is ~10 m in height (measured from the ground to its diapiric apex), metres to decametres deep below ground (based on borehole data) and decametres back from the exposure **(see, Fig. 3)**. Ice-wedges are observed in the overburden. Slight depressions above the ice-wedges ***(red arrows)*** demarcate ***HCP*** margins. At this location the ***HCPs*** are degradational landforms that form when polygon-margin ice wedges melt and depress the overlying shoulders. Geologists to the right of the ***MI*** provide scale. Photo credit: R. Soare.

What on Earth/Mars?; ice-complex stratigraphy and associated boundary conditions: Ice-rich thermokarst/ground ice (not shown here), retrogressive thaw-slumps and the derived exposure of tabular ***MI*** are commonplace along beach fronts in the ***TC*** **[e.g. 4-8].** Typically, the ***MI*** exhibits horizontal foliation **(Fig. 2)**. This is the result of sediment-rich bands melting therein **[e.g. 7]**.

Fig. 3. Oblique view of the thaw slumps at ***PP***. White box locates the ***MI*** exposure shown in **Fig. 2.** Note the outcrop of polygonised terrain at the extreme bottom-end of the photo. Photo credit: R. Soare.

Despite ~50 years of observation, speculation and surmisal, explanations concerning the origin of the ***MI*** remain equivocal. The leading hypotheses comprise intra-sedimentary, i.e. segregation and intrusive, ice **[e.g. 4, 6]**; sub-glacial meltwater **[e.g. 5]**, buried surface-ice, i.e. glacial ice **[e.g. 5-6]**. Age dating suggests that the ***MI*** itself is thousands of years old and could

have formed very late in the Pleistocene Era or early on in the Holocene Epoch **[e.g. 4-6]**.

The ***MI*** overburden comprises a clayey diamicton, overlain by a shallow active-layer **(Fig. 2)**. In turn, the active-layer is punctuated by ***HCPs*** ~5-15 m in diameter at the surface. Often, the ***HCPs*** are underlain at the margins by vertically foliated and metres-deep ice wedges **(Figs. 2-3)**. Each vertical leaf represents one cycle of growth/aggradation.

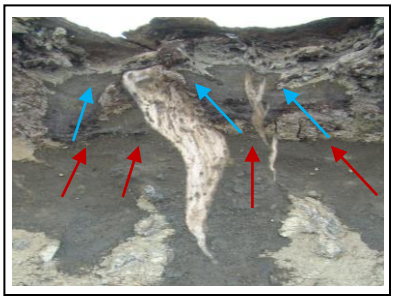

Fig. 4. Cross-sectional profile of ice-wedges at ***PP***. **a)** Here, as in **Fig. 1.**, the two ice-wedges closest to the surface underlie two surface depressions that comprise ***HCP*** margins. Note, a third ice-wedge resides directly below the near-surface wedge on the right and represents an earlier generation of wedge formation. Earlier post-glacial thaw unconformity #1 (***burgundy arrows***). Later post-glacial thaw unconformity #2 (***blue arrows***). Photo credit: R. Soare.

As noted above [**Fig. 2** caption], many of the ***TC HCPs*** are degradational landforms underlain by marginal ice-wedges. Sand wedges also underlie some ***HCP*** margins. Whereas the icy ***HCPs*** originate and develop under "*warmish*" mean temperatures **[e.g. 7]**, high-centred sand-wedge polygons are the work of aeolian erosion.

Icy ***TC LCPs*** are aggradational landforms that develop as meltwater accumulates episodically at polygon margins by the freeze-thaw cycling of water **[e.g. 5, 7]**. Sand-wedge ***LCPs*** are less common in the region and aggrade by aeolian accumulation. Both of these polygonised terrain types are the necessary antecedents of ***HCPs*** in cold-climate non-glacial regions on Earth.

Fig. 5. Ice/sand wedge and sand-wedge ***HCPs*** in the ***TC*** **[9]**. Note the slight depression in the overburden above the ice/sand wedge on the left and the sand wedge on the right.

Absent of a pick and shovel, validating the presence of ice vs sand wedges at polygons margins beneath the Martian surface is difficult. However, we have shown that when ***LCP/HCP*** assemblages occur on their own on Mars or in conjunction with thermokarst-like depressions there is a high degree of statistical probability that the margins are or have been underlain by ice wedges **[10]**.

Also of note in the ***PP MI***/overburden cross-sections is the presence of multiple thaw-unconformities i.e. sedimentary-boundaries that denote separate (paleo) active-layers and separate periods of ice-wedge formation.

Discussion: Two of the three principal hypotheses on the origin of the ***TC MI*** are based on the freeze-thaw cycling of water. The third hypothesis assumes that the ***MI*** is buried glacial-ice. The open-ended discussions that persist on the origin of ***MI*** at the ***TC*** attest to the difficulties associated in identifying one unique formation-hypothesis above the others even through decades of work Earth-based ***MI***.

However, two keynotes can be derived from these hypotheses and discussions that could be relevant to the scarp-face exposures of ***MI*** on Mars:

1) Regardless of the absolute age or the process(es) that formed the ***MI*** at ***PP***, the ***MI*** overburden and ensconced ice-wedge polygons present at least two periods of thaw that followed the ***MI's*** origin. This, along with regional ice-rich thermokarst, point to mean-temperature variances and boundary conditions in the ***TC*** that were substantially different from those associated with the origin of the underlying ***MI***.

2) Similarly, the polygonised (metres-thick) overburden and the polygonised terrain in which the icy exposures on Mars are ensconced, as well as the possibly ice-rich thermokarst-like depressions that populate the surrounding landscape, could be indicative of temperature variances and boundary conditions that differ substantially from those associated with the emplacement of the buried and partially exposed ***MI*** on Mars.

References: **[1]** Dundas, C.M. et al. (2018). *Science* 359, 199-201, 10.1126/science.aao1619. **[2]** Harish. et al. (2020). *Geophys. Res. Lett.* 47e2020(GL 089057), doi.org/10.1029/2020GL089057. **[3]** Dundas, C.M. et al. (2021). *J. Geophys. Res.* 126, doi.org/10.10 29/2020JE006617. **[4]** Mackay, J.R. (1971). *Can. J. Earth Sci.* 8(4), 397-422. **[5]** Rampton, V.N. (1991). *Permafr. Periglac.* 2, 163-165. **[6]** Mackay, J.R., Dallimore, S. (1992). *Can. J. Earth. Sci.* 29(6), 1235-1249. **[7]** Soare, R.J. et al. (2011). *GSA Special Paper* 483, 2 03-218, doi:10.1130/2011.2483(13). **[8]** Wetterich. S. et al. (2019). *Quat. Res.* 1-19, doi:10.1017/qua.2019.6. **[9]** Murton, J.B. et al. (2000). *Quat. Sci. Rev.* 19, 899-922. **[10]** Soare, R.J. et al. (2021). *Icarus* 358(114208), doi.org/10.1016/j.icarus.2020.114208.